CHAPTER

12

Fluorescence methods for analysis of interactions between Ca^{2+} signaling, lysosomes, and endoplasmic reticulum

David L. Prole, Cristina I. López-Sanjurjo, Stephen C. Tovey, Colin W. Taylor[1]

Department of Pharmacology, University of Cambridge, Cambridge, UK

[1]*Corresponding author: E-mail: cwt1000@cam.ac.uk*

CHAPTER OUTLINE

Abstract

The endoplasmic reticulum (ER) is both the major source of intracellular Ca^{2+} for cell signaling and the organelle that forms the most extensive contacts with the plasma membrane and other organelles. Lysosomes fulfill important roles in degrading cellular materials and in cholesterol handling, but they also contribute to Ca^{2+} signaling by both releasing and sequestering Ca^{2+}. Interactions between ER and other Ca^{2+}-transporting membranes, notably mitochondria and the plasma membrane, often occur at sites where the two membranes are closely apposed, allowing local Ca^{2+} signaling between them.

Methods in Cell Biology, Volume 126, ISSN 0091-679X, http://dx.doi.org/10.1016/bs.mcb.2014.10.024

These interactions are often facilitated by scaffold proteins. Recent evidence suggests similar local interactions between ER and lysosomes. We describe simple fluorescence-based methods that allow the interplay between Ca^{2+} signals, the ER, and lysosomes to be examined.

1. ER, LYSOSOMES, AND Ca^{2+} SIGNALING

Experimental analyses of Ca^{2+} signaling have seen different membranes move in and out of the limelight. For many years, beginning with the first evidence that Ca^{2+} regulates cellular activities (Ringer, 1883), Ca^{2+} influx across the plasma membrane was assumed to be entirely responsible for increases in cytosolic free Ca^{2+} concentration ($[Ca^{2+}]_c$). These Ca^{2+} entry pathways are important, indeed the store-operated Ca^{2+} entry (SOCE) pathway is almost ubiquitous (Putney, 1997), but Ca^{2+} channels in the plasma membrane rarely work in isolation. The demonstration that many extracellular stimuli evoke transient increases in $[Ca^{2+}]_c$ in the absence of extracellular Ca^{2+} focused attention on intracellular Ca^{2+} stores. Mitochondria were the first suspects (Exton, 1980), but when they were shown to accumulate Ca^{2+} only when bathed in $[Ca^{2+}]$ that considerably exceeded the $[Ca^{2+}]_c$ measured in cells, attention switched to the endoplasmic reticulum (ER). It is now clear that the ER (or sarcoplasmic reticulum in muscle) is the major intracellular Ca^{2+} store from which extracellular stimuli release Ca^{2+} (Burgess, McKinney, Fabiato, Leslie, & Putney, 1983; Streb, Irvine, Berridge, & Schulz, 1983). Sarco/endoplasmic reticulum Ca^{2+}-ATPases (SERCA) allow active uptake of Ca^{2+} from the cytosol into the lumen of the ER using the energy provided by ATP hydrolysis. The affinity of SERCAs for Ca^{2+} ($K_m \sim 0.5-2\ \mu M$) (Lytton, Westlin, Burk, Shull, & MacLennan, 1992) is similar to the $[Ca^{2+}]_c$ of an unstimulated cell, allowing the ER to sequester Ca^{2+}. This generates a high luminal $[Ca^{2+}]$ (typically $>500\ \mu M$) (Suzuki et al., 2014) and so a steep $[Ca^{2+}]$ gradient across the ER membrane. Regulated opening of Ca^{2+}-permeable channels within the ER membrane, the most abundant of which are inositol 1,4,5-trisphosphate receptors (IP_3R, which are activated by IP_3) and ryanodine receptors (RyR) (Taylor & Dale, 2012), allows Ca^{2+} to flow rapidly back into the cytosol down its concentration gradient, generating the cytosolic Ca^{2+} signals that regulate cellular activities (Berridge, 1997). IP_3R and RyR share many structural and functional characteristics (Seo et al., 2012), most notably their regulation by cytosolic Ca^{2+} (Taylor & Dale, 2012). The ability of Ca^{2+} to stimulate gating of these intracellular Ca^{2+} channels via Ca^{2+}-induced Ca^{2+} release (CICR) is important because CICR mediates regenerative propagation of Ca^{2+} signals from the ER (Berridge, Lipp, & Bootman, 2000; Marchant, Callamaras, & Parker, 1999) and it allows the ER to respond to Ca^{2+} provided by channels in other membranes, including lysosomes (Brailoiu et al., 2010; Calcraft et al., 2009; Lam & Galione, 2013). The Ca^{2+} content of the ER, which is itself an important regulator of Ca^{2+} entry across the plasma membrane via SOCE (Lewis, 2012), is thus determined by the competing activities of SERCAs and Ca^{2+}-permeable channels. The approximately 50,000-fold greater rate of Ca^{2+} transport

through intracellular Ca^{2+} channels like IP_3R ($\sim 5 \times 10^5$ Ca^{2+}/s) (Vais, Foskett, & Mak, 2010) relative to SERCA (~ 10 Ca^{2+}/s) (Lytton et al., 1992), which is typical of the difference between channels and pumps, highlights the importance of Ca^{2+}-permeable channels in rapidly generating substantial local changes in $[Ca^{2+}]_c$.

The rush to embrace ER Ca^{2+} stores caused mitochondria to be neglected until they were shown to accumulate Ca^{2+} when their proximity to Ca^{2+} channels provided local $[Ca^{2+}]$ sufficient to allow uptake by the mitochondrial uniporter (Rizzuto, Brini, Murgia, & Pozzan, 1993). So began a resurgence of interest in both the contributions of mitochondria to shaping and decoding cytosolic Ca^{2+} signals (Rizzuto, De Stefani, Raffaello, & Mammucari, 2012), and the importance of local Ca^{2+}-mediated signaling between membranes. The latter is possible because abundant cytosolic Ca^{2+} buffers cause Ca^{2+} to diffuse slowly within cytosol, thereby allowing high $[Ca^{2+}]_c$ to persist around the mouths of Ca^{2+} channels for as long as they remain open (Konieczny, Keebler, & Taylor, 2012; Shuai & Parker, 2005). In many cases, proteins that tether one membrane to another facilitate the local interactions between membranes (Helle et al., 2013; Prinz, 2014).

Acidic organelles, and particularly lysosomes, are the most recent organelles to be implicated in Ca^{2+} signaling, with evidence suggesting that they can both release Ca^{2+} to the cytosol and accumulate Ca^{2+} from it (Morgan, Platt, Lloyd-Evans, & Galione, 2011). Ca^{2+} uptake by lysosomes requires the pH gradient established across the lysosomal membrane by the ubiquitous and highly regulated H^+-pumping vacuolar-type H^+-ATPase (V-ATPase), a relative of the F_0F_1 ATP synthase responsible for mitochondrial ATP synthesis. But neither the properties nor the molecular identities of mammalian lysosomal Ca^{2+} uptake systems are known (Morgan et al., 2011; Patel & Docampo, 2010). Different studies report hugely variant affinities for Ca^{2+} uptake by mammalian lysosomes (Klemper, 1985; Lemons & Thoene, 1991; Lopez Sanjurjo, Tovey, Prole, & Taylor, 2013). By analogy with plants, where the vacuole (analogous to animal lysosomes) is the major intracellular Ca^{2+} store, a reasonable candidate for Ca^{2+} uptake into mammalian lysosomes may be via Ca^{2+}/H^+ exchangers, analogous to plant vacuolar CAX proteins (but different from them, because animal genomes lack sequences similar to plant CAX proteins) (Morgan et al., 2011).

A major advance has been the realization that lysosomal membranes also express Ca^{2+}-permeable channels such as P2X4 receptors (Huang et al., 2014), several members of the transient receptor potential (TRP) channel superfamily (e.g., TRPML1 and TRPM2) (Dong, Wang, & Xu, 2010), and two-pore channels (TPC). The latter may be regulated by nicotinic acid adenine dinucleotide phosphate (NAADP), Mg^{2+}, phosphatidylinositol 3,4-bisphosphate, pH, membrane potential, mTORC1, and other protein kinases (Calcraft et al., 2009; Cang et al., 2013; Jha, Ahuja, Patel, Brailoiu, & Muallem, 2014; Pitt, Lam, Rietdorf, Galione, & Sitsapesan, 2014; Wang et al., 2012). Furthermore, Ca^{2+} release via lysosomal channels can be amplified by CICR mediated by either IP_3R or RyR within ER membranes (Brailoiu et al., 2010; Calcraft et al., 2009; Lee, 2005; Patel et al., 2011). Hence for lysosomes, as with other membranes that contribute to Ca^{2+} signaling, local interactions with the ER,

mediated by close contacts between membranes at membrane contact sites (MCS), are an important feature (Lopez Sanjurjo et al., 2013; Morgan et al., 2013). However, the roles of MCS extend far beyond Ca^{2+} signaling because they are also important in mediating lipid exchanges, in facilitating enzyme−substrate interactions between membranes, and in partitioning organelles between dividing cells (Helle et al., 2013; Prinz, 2014). Other contributors to this volume address the possible identities of proteins involved in tethering lysosomes to other membranes (Friedman, Dibenedetto, West, Rowland, & Voeltz, 2013; Kilpatrick, Eden, Schapira, Futter, & Patel, 2013; Van der Kant & Neefjes, 2014). The properties of lysosomal ion channels, the extent to which they are Ca^{2+}-permeable, and the methods available for their analysis are also discussed elsewhere in this volume. In this chapter, we describe the application of fluorescence techniques to address the interplay between Ca^{2+} signaling, ER, and lysosomes.

2. PHARMACOLOGICAL TOOLS

Two widely used membrane-permeant inhibitors allow selective inhibition of SERCA. The plant sesquiterpene lactone, thapsigargin, irreversibly inhibits SERCA (Michelangeli & East, 2011; Sagara & Inesi, 1991), while cyclopiazonic acid causes reversible inhibition (Demaurex, Lew, & Krause, 1992). Each depletes the ER of Ca^{2+} as basal leaks proceed unopposed by Ca^{2+} pumping. Selective activation of IP_3R is usually achieved by stimulation of receptors coupled to phospholipase C (Lopez Sanjurjo et al., 2013). More direct means of activating IP_3R include a membrane-permeant esterified form of IP_3 (IP_3-BM, IP_3 hexakis(butyryloxymethyl)) that crosses the plasma membrane and then stimulates IP_3R once it has been de-esterified by endogeneous esterases (Li, Schultz, Llopis, & Tsien, 1997; Tovey, Goraya, & Taylor, 2003). Better temporal control of IP_3 delivery is provided by flash-photolysis of caged IP_3, which can either be microinjected (c-IP_3-P4, IP_3 with a photolabile nitrophenyl ester occluding the 4-phosphate) or loaded into cells as an esterified precursor of caged-IP_3 (ci-IP_3/PM, available from Sichem, Bremen, Germany) (Smith & Parker, 2009). Cleavage of the ester groups of ci-IP_3/PM unmasks caged-IP_3, from which ultraviolet light releases the active ligand. It is worth noting that photolysis of c-IP_3-P4 releases IP_3 itself, whereas photolysis of ci-IP_3 (derived from ci-IP_3/PM) releases a modified form of IP_3 that is more slowly metabolized. Unfortunately, there are no reliable, selective, and membrane-permeant antagonists of IP_3R (Saleem, Tovey, Molinski, & Taylor, 2014). Caffeine, which has many additional effects, is commonly used to activate RyR, while high concentrations of ryanodine are inhibitory. Additional inhibitors of IP_3R (Saleem et al., 2014) and RyR (Mackrill, 2010), and their limitations are described elsewhere.

Unsurprisingly, given the unknown identity of mammalian lysosomal Ca^{2+} sequestration mechanisms (Section 1), there are no known direct inhibitors of lysosomal Ca^{2+} uptake, but selective inhibitors of the V-ATPase provide effective means of indirectly inhibiting lysosomal Ca^{2+} sequestration. The macrolides, bafilomycin

A_1 (Drose & Altendorf, 1997; Yoshimori, Yamamoto, Moriyama, Futai, & Tashiro, 1991), and concanamycin A (Drose & Altendorf, 1997), selectively inhibit the V-ATPase via noncovalent binding (Marshansky & Futai, 2008), without affecting the related F_0F_1 ATP synthase. For these inhibitors to release Ca^{2+} rapidly from lysosomes, basal leaks of H^+ (and counterion) must be sufficient to dissipate the pH gradient and so prevent further Ca^{2+} uptake, and a basal Ca^{2+} leak must be sufficient to allow Ca^{2+} to escape. It is worth noting that changes in lysosomal pH also affect luminal Ca^{2+} buffering, with a rise in pH increasing the buffering capacity (as H^+ less effectively competes with Ca^{2+} for buffers), thereby reducing the luminal free [Ca^{2+}] and the Ca^{2+} gradient across the lysosome membrane. Protonophores (e.g., FCCP) or NH_4Cl also dissipate lysosomal H^+ gradients, but these tools lack selectivity in intact cells (Christensen, Myers, & Swanson, 2002; Morgan & Galione, 2007). A recent review (Morgan et al., 2011) provides a thoughtful analysis of interactions between lysosomal pH and Ca^{2+} handling. Two alternative means of disrupting lysosomal behavior are also useful. The dipeptide, glycyl-L-phenylalanine 2-naphthylamide (GPN) is a substrate of the lysosomal protease, cathepsin C, and when cleaved within lysosomes it causes their selective lysis by osmosis (Churchill et al., 2002; Jadot, Colmant, Wattiaux-De Coninck, & Wattiaux, 1984; Lopez Sanjurjo et al., 2013). Vacuolin-1 is a small triazine-based molecule originally identified from a compound library; it causes fusion of lysosomes by mechanisms that remain unresolved (Huynh & Andrews, 2005). All three pharmacological approaches to interfere with lysosomal Ca^{2+} handing—inhibition of V-ATPase (bafilomycin A_1, concanamycin), GPN and vacuolin-1—are applicable to intact cells and have found widespread application.

3. FLUORESCENCE METHODS

Absorption of a photon by a fluorescent molecule moves an electron from its ground state (S_0) to an excited singlet state (S_2). Over a few ns, some of the absorbed energy is then dissipated before the electron returns (from S_1) to its ground state, emitting a photon with less energy (longer wavelength) than the one that caused excitation (Lakowicz, 2006). It would be hard to over-state the impact of fluorescence methods in biology, and the reasons are numerous (Giepmans, Adams, Ellisman, & Tsien, 2006; Zhang, Campbell, Ting, & Tsien, 2002). Fluorescence methods can be relatively noninvasive; excitation and detection of fluorescence at two different wavelengths provides specificity; chemically and biologically derived probes are available in every imaginable hue, allowing simultaneous recording from different probes; fluorescence microscopy provides the resolution needed to examine cell behaviors at the most relevant temporal and spatial scales; genetically encoded fluorescent proteins allow subcellular targeting and optimization of probes by directed evolution; fluorescent probes can be engineered to sense or manipulate many biologically important molecules; and fluorescent reporters lend themselves to high-throughput analyses (e.g., for pharmacological or siRNA and/or gene-knockdown screening).

All fluorescence techniques use a light source to excite the sample and then emitted light is captured after selection of specific wavelength(s) using appropriate filters. For wide-field fluorescence microscopy, the sample is illuminated, and emitted fluorescence is detected with, for example, a charge-coupled device (CCD). Wide-field imaging is simple, inexpensive, sensitive, and compatible with a variety of light sources, but the resolution particularly in the z-dimension is compromised by collection of light from outside the focal plane. A modest improvement in xy-resolution and a large improvement in z-resolution are provided by confocal microscopy, where a pinhole positioned in the light path removes light emitted from outside the focal plane. Laser scanning confocal microscopy (LSCM) scans a laser beam across the sample and detects emitted light using photomultiplier tubes or photodiodes. LSCM is very sensitive and provides images with high spatial resolution in x, y, and z dimensions, but scanning light across the sample results in relatively slow capture rates. An alternative is the spinning-disk confocal microscope, which utilizes multiple pinholes (or slits) to near-simultaneously illuminate and collect light from the entire field. This enables detection using a CCD or electron multiplying CCD (EM-CCD), allowing higher speed imaging, but with a slight loss in z-resolution. Further improvements in z-resolution come with total internal reflection fluorescence (TIRF) microscopy, where a laser beam generates an evanescent wave at the interface between two media with different refractive indices. For biological imaging, this is usually the interface between a coverslip and the overlying aqueous medium (Martin-Fernandez, Tynan, & Webb, 2013). Because the intensity of the evanescent wave decays exponentially from the interface, fluorophores are illuminated only if they fall within 100−300 nm of the coverslip surface; the depth of illumination varies with the incident angle and wavelength of the illuminating light (Lakowicz, 2006; Martin-Fernandez et al., 2013). TIRF microscopy, which is relatively straightforward, thereby provides unparalleled z-resolution and the low background needed for single-molecule imaging. Most TIRF microscopy, including that described herein, delivers light from a laser to the sample via an objective with high numerical aperture (NA) ("objective-based" TIRF) (Martin-Fernandez et al., 2013). However, TIRF microscopy can only visualize cellular components that are close to the plasma membrane. Nevertheless, because many IP_3-evoked Ca^{2+} events (Smith & Parker, 2009) and interactions between fluorescently labeled ER and lysosomes (Lopez Sanjurjo et al., 2013) occur close to the plasma membrane, TIRF microscopy allows these behaviors to be observed with unparalleled z-resolution.

The xy-resolution of conventional optical microscopes is limited by the diffraction of light, which for objectives with high NA limits resolution to about half the wavelength of the excitation light. This resolution limit (typically ~200 nm) is substantially greater than the dimensions of membranes, MCS, and proteins. Until recently, the only means of breaking this diffraction limit was to use electromagnetic radiation with much shorter (and more damaging) wavelengths (e.g., electron microscopy) that are incompatible with live-cell

imaging (Kilpatrick et al., 2013). Recently, however, several techniques have been developed to break the optical diffraction limit. These "super-resolution" methods can be broadly divided into two categories. The first category modifies the excitation light to provide either patterned illumination, from which an image is derived by computational analysis of the resulting diffraction pattern (structured illumination), or it restricts fluorescence to a spot smaller than the diffraction limit by quenching fluorescence from the periphery of the excited spot (stimulated emission depletion, STED, microscopy) (Han, Li, Fan, & Jiang, 2013). The second major set of approaches excites only a small fraction of fluorescent molecules in each image, allowing each probe to be precisely localized. The fluorophores are then bleached, before visualizing the next subset. After many such cycles a complete fluorescence image is reconstructed by overlaying the images of the sparse fluorescence points. Stochastic optical reconstruction microscopy (STORM, which commonly uses fluorescently tagged antibodies) and photo-activated localization microscopy (PALM, which requires the target to be tagged with a photoactivatable probe) are two commonly used variants of this approach, but there are now many others (Han et al., 2013). Because these super-resolution methods require collection of many serial images to reconstruct the final image, a limitation is their speed, although this is rapidly improving (Shim et al., 2012). Super-resolution microscopy has provided images of lysosomes in fixed (Betzig et al., 2006) and live cells (Shim et al., 2012), but it has not yet addressed interactions between lysosomes and ER. In this chapter, we discuss only TIRF microscopy. Figure 1 compares images of the same COS-7 cell expressing an ER-targeted protein viewed by wide-field and TIRF microscopy to illustrate the benefits of the latter.

4. FLUORESCENCE TOOLS FOR ANALYSIS OF LYSOSOMES

Our focus on Ca^{2+} signaling, ER, and lysosomes identifies the need for fluorescent probes for reporting $[Ca^{2+}]$ and organelle identity. Conventional, BAPTA-based Ca^{2+} indicators (e.g., fura 2, fluo 4, etc.) in their acetoxymethyl (AM) ester forms allow facile loading of cells with fluorescent reporters of $[Ca^{2+}]_c$. It is, however, necessary to optimize loading protocols to avoid compartmentalization of the indicator within organelles or its extrusion across the plasma membrane (Bootman, Rietdorf, Collins, Walker, & Sanderson, 2014). The properties of these indicators, which embrace a range of affinities for Ca^{2+} and fluorescent spectra, are available at: http://www.lifetechnologies.com and http://www.teflabs.com. Ca^{2+} indicators based on fluorescent proteins provide opportunities for genetic targeting, and they are available with a range of Ca^{2+} affinities, and as both ratiometric and single-wavelength reporters. These probes have been used to report $[Ca^{2+}]_c$ and ER luminal $[Ca^{2+}]$ (Suzuki et al., 2014), but there are considerable problems in extending their use to measurement of lysosomal $[Ca^{2+}]$ (Section 5). The interplay between lysosomal pH and Ca^{2+} signaling (Section 1) presents a need to measure lysosomal

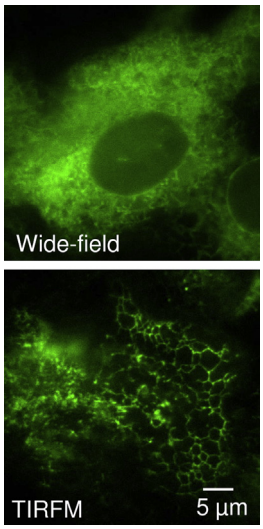

FIGURE 1

Comparison of wide-field and TIRF images. Two images from the same field show a COS-7 cell expressing CatchER (a GFP-based Ca^{2+}-sensor targeted to the ER lumen) (Tang et al., 2011) viewed by wide-field or TIRF microscopy. (See color plate)

Reproduced with permission from Lopez Sanjurjo et al. (2013).

and cytosolic pH reliably (see Sections 5 and 6). Additional approaches to measuring lysosomal pH are described elsewhere in this volume.

A second need is to identify, by fluorescence, ER and lysosomes. Here, lysosomes present two advantages: they are the most acidic of organelles and they are the compartment in which endocytosed materials accumulate. Hence, fluorescent probes that accumulate in acidic environments (e.g., LysoTrackers, Acridine Orange, quinacrine) provide simple means of identifying lysosomes in live cells, albeit with imperfect specificity (Pierzynska-Mach, Janowski, & Dobrucki, 2014). Pulse-chase protocols with endocytosed dextran-fluorophore conjugates provide an alternative means of fluorescently labeling the lumen of the lysosome (Section 8). Fluorescent proteins targeted to organelles by signal sequences or by their attachment to organelle-specific proteins provide additional means of identifying ER and lysosomes for live-cell imaging. Attachment of fluorescent proteins (e.g., EGFP, mCherry) to lysosome-associated protein 1 (LAMP1) identifies lysosomes, while green fluorescent protein (GFP) targeted to the outer leaflet of the ER (GFP-ER) (Wozniak et al., 2009) or tagged versions of such ER proteins as IP_3R and SERCA identify ER. Figure 2 shows images of a live COS-7 cell transfected to express GFP-IP_3R3 (ER) or GFP-ER, and LAMP1-mCherry (lysosomes). Our use of these methods to track dynamic relationships between ER and lysosomes is described in Section 8.

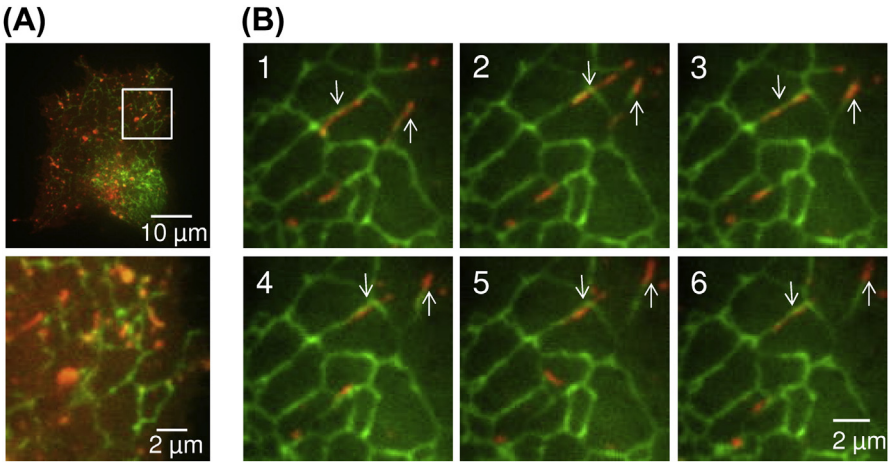

FIGURE 2

Intimate and dynamic association between lysosomes and ER. (A) Images of a COS-7 cell co-transfected with GFP-IP_3R3 (ER, green) and LAMP1-mCherry (lysosomes, red) and visualized by TIRF microscopy show the intimate relationship between ER and lysosomes. Lower panel shows a magnified image of the boxed region. (B) Time-lapse images (16 s between images) of a live COS-7 cell co-transfected with LAMP1-mCherry (red) and GFP-ER (green) (Wozniak et al., 2009). Images show a lysosome moving along the ER (downward arrows) and another lysosome moving concomitantly with the leading edge of an extending ER tubule (upward arrows). (See color plate)

5. Ca^{2+} SIGNALING AND LYSOSOMES: TOOLS AND PRACTICAL PROBLEMS

The lumen of the lysosome is an exceptionally hostile environment in which to measure free [Ca^{2+}]. The acidic pH (~pH 4.5) (Ishida, Nayak, Mindell, & Grabe, 2013) massively reduces the Ca^{2+} affinity of indicators, and even small changes in pH, such as are expected to accompany Ca^{2+} uptake and/or release by lysosomes (Lopez Sanjurjo et al., 2013; Morgan & Galione, 2007), may substantially change the apparent affinity of the indicator. It thus becomes difficult to disentangle changes in pH from changes in [Ca^{2+}] (Christensen et al., 2002). Lysosomal proteases present a second problem. They effectively forbid the use of genetically encoded protein-based Ca^{2+} indicators within lysosomes. However, an advantage of lysosomes is that they are the terminal compartments for endocytosed materials, and this allows indicators to be sent to the lumen of lysosomes by endocytosis using pulse-chase protocols (Christensen et al., 2002; Lloyd-Evans et al., 2008; Lopez Sanjurjo et al., 2013). The same methods can be used for delivery of dextran-conjugated pH indicators to lysosomes (e.g., fluorescein, Oregon Green) or inert conjugates (e.g., Texas Red, Alexa-Fluor dyes) for ratiometric analyses.

Dextran conjugates of organic Ca^{2+} indicators (fura 2, low-affinity rhod 2 or Oregon Green BAPTA), each with an affinity (K_D^{Ca}) of ~500 μM at pH 4.5 (Christensen et al., 2002; Lloyd-Evans et al., 2008), have been used to report $[Ca^{2+}]$ within lysosomes. Endocytic uptake of the conjugate, followed by a chase period to allow its movement from early endosomes allows effective delivery of the indicator to lysosomes (Christensen et al., 2002; Gerasimenko, Tepikin, Petersen, & Gerasimenko, 1998; Lloyd-Evans et al., 2008; Lopez Sanjurjo et al., 2013). In our experience, the approach can be compromised by ineffective coupling of dextran to the indicator in some commercial preparations. There are two remaining technical problems. First, the fluorescence of some Ca^{2+} indicators, Oregon Green BAPTA, for example, is directly and substantially affected by pH (Figure 3). Second, the massive effects of pH on K_D^{Ca} demand meticulous pH corrections if measurements of lysosomal $[Ca^{2+}]$ are accompanied by lysosomal pH changes. Dextran-conjugated low-affinity rhod 2 (no longer commercially available) was, for example, used to measure lysosomal $[Ca^{2+}]$ in cells expressing mutant

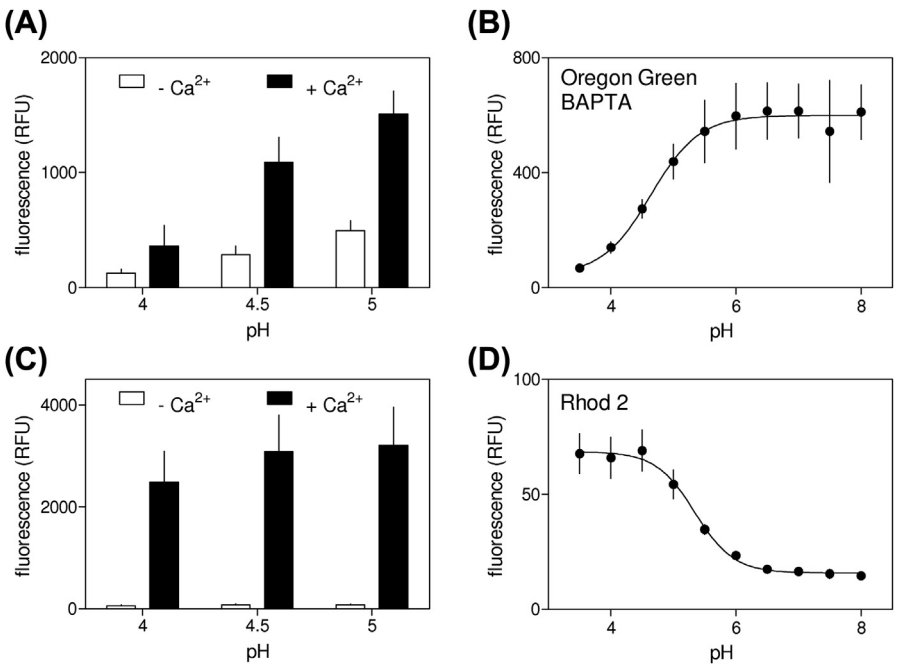

FIGURE 3

Effects of pH and Ca^{2+} on two dextran-conjugated indicators. Fluorescence emission from Oregon Green BAPTA (A, B) and Rhod 2 (C, D) recorded in media at different pH and with either 100 mM $CaCl_2$ or EGTA. The effects of pH in the absence of Ca^{2+} (B and D) demonstrate appreciable effects of low pH on the fluorescence of Oregon Green BAPTA, but only small effects on Rhod 2. RFU, relative fluorescence units.

Niemann-Pick type 1 protein (NPC1), and because lysosomal pH was the same in normal and mutant cells, the conclusion that lysosomal [Ca^{2+}] is reduced in the mutant cells was not dependent on the accuracy of the pH correction for K_D^{Ca}. Where lysosomal pH changes do occur, it is more difficult to distinguish unambiguously whether changes in fluorescent Ca^{2+} indicators are due to changes in lysosomal free [Ca^{2+}], changes in K_D^{Ca} or direct effects of pH on the fluorescence of the indicator.

Targeting of protein-based indicators to the lumen of lysosomes may be impracticable, but a low-affinity indicator expressed on the cytosolic surface of lysosomes would provide opportunities to measure local Ca^{2+} signals arising from lysosomal Ca^{2+} channels or apposed ER Ca^{2+} channels. McCue et al. used a cameleon (YCam3.6), in which intramolecular association of Ca^{2+}-calmodulin with M13 peptide brings terminal fluorescent proteins (CFP and cpYFP) together to allow Förster resonance energy transfer (FRET) (Nagai, Yamada, Tominaga, Ichikawa, & Miyawaki, 2004), and targeted it to the cytosolic surface of lysosomes via LAMP1. Although LAMP1-YCam3.6 was effectively targeted to lysosomes, its affinity ($K_D^{Ca} = 250$ nM) is too high to selectively report local high [Ca^{2+}] effectively. Nevertheless, the study demonstrates the potential utility of Ca^{2+} indicators targeted to the cytosolic surface of lysosomes as a means of selectively reporting changes in $[Ca^{2+}]_c$ near-lysosomes.

The simple message is that analyses of lysosomal Ca^{2+} signaling are hampered by the lack of straightforward and reliable means of measuring [Ca^{2+}] within lysosomes. In subsequent sections, we provide protocols for three different approaches to analysis of interactions between lysosomes, ER and Ca^{2+} signaling. All rely on measurements of fluorescence. The first describes single-cell analyses of cytosolic Ca^{2+} signals (Section 6), the second allows high-throughput analyses of the effects of lysosomes on cytosolic Ca^{2+} signals in populations of cultured cells (Lopez Sanjurjo et al., 2013) (Section 7), and the third describes methods for tracking dynamic relationships between ER and lysosomes (Section 8).

6. SINGLE-CELL ANALYSES OF CYTOSOLIC Ca^{2+} SIGNALS

6.1 MATERIALS

1. Calcium Calibration Buffer Kit #1 and fura 2-AM (Life Technologies, Paisley, UK). Pluronic F127 (Sigma, Poole, UK). Ionomycin (Merck Eurolab, Nottingham, UK)
2. 22-mm diameter round glass coverslips coated with poly-L-lysine
3. HBS (HEPES-buffered saline): NaCl 135 mM, KCl 5.9 mM, $MgCl_2$ 1.2 mM, $CaCl_2$ 1.5 mM, HEPES 11.6 mM and glucose 11.5 mM, pH 7.3. Ca^{2+} is omitted from nominally Ca^{2+}-free HBS, and replaced by BAPTA (10 mM, 1,2-bis(*o*-aminophenoxy)ethane-N,N,N′,N′-tetraacetic acid, Molekula, Dorset, UK) in Ca^{2+}-free HBS

4. Carbachol, DMSO and vacuolin (Sigma, Poole, Dorset), bafilomycin A_1 (AG Scientific, California, USA) and GPN (Bachem, St Helens, UK)
5. Inverted fluorescence microscope

The method is similar to that described previously (Tovey, Dedos, Taylor, Church, & Taylor, 2008). Plate HEK-293 or COS-7 cells onto poly-L-lysine-coated glass coverslips at densities that allow them to reach confluence in 2 days. Load cells with fura 2-AM (2 μM, 1 h, 20 °C, final DMSO concentration 0.2%, protected from light) in HBS supplemented with Pluronic F127 (0.02%). After loading, incubate cells in HBS for 1 h (20 °C, protected from light) to allow de-esterification of the indicator. Wash cells with fresh HBS to remove extracellular dye. Place the coverslip on the stage of an inverted fluorescence microscope. Excite cells alternately with light at wavelengths of 340 nm and 380 nm, and collect fluorescence emitted at 510 nm. At the end of the experiment, add $MnCl_2$ (10 mM, which quenches all fura 2 fluorescence) with ionomycin (1 μM, an ionophore that mediates Mn^{2+} transport into the cytosol). For analysis, select regions of interest (ROI, e.g., single cells) and average the fluorescence values for all pixels within the ROI at each collection interval. For each measurement, subtract the autofluorescence value determined in the presence of Mn^{2+} before calculating fluorescence ratios (F_{340}/F_{380}). Fluorescence signals can then be calibrated to $[Ca^{2+}]_c$ (Grynkiewicz, Poenie, & Tsien, 1985):

$$\left[Ca^{2+}\right]_c = K_D \frac{R - R_{min}}{R_{max} - R} \cdot \frac{F_{max}}{F_{min}}$$

where R, R_{min}, and R_{max} are the background-corrected fluorescence ratios (F_{340}/F_{380}) for the experimental measurement of Ca^{2+}-free or Ca^{2+}-saturated fura 2, respectively. F_{max} and F_{min} are the fluorescence intensities recorded at 380 nm, for Ca^{2+}-free and Ca^{2+}-saturated fura 2. K_D is the equilibrium dissociation constant for fura 2-Ca^{2+} (224 nM, determined in vitro at 22 °C, pH 7.2) (Grynkiewicz et al., 1985). An alternative method is to generate a standard curve from commercially available Ca^{2+}-standard solutions supplemented with fura 2 and so generate a look-up table for fluorescence ratios versus $[Ca^{2+}]_c$.

For HEK-293 cells, a typical experiment might include an analysis of the effects of carbachol (1 mM), which activates M3 muscarinic receptors and thereby phospholipase C, on the peak increase in $[Ca^{2+}]_c$ alone or after perturbation of lysosomal function (Figure 4(A)). The latter could include inhibition of the V-ATPase (bafilomycin A1, 1 μM, 1 h), perforation of lysosomes (GPN, 200 μM, 30 min), or fusion of lysosomes (vacuolin-1, 10 μM, 1 h) (Lopez Sanjurjo et al., 2013). Because many of the perturbations of lysosomes risk altering cytosolic pH (and thereby the K_D^{Ca} of cytosolic fura 2), important controls include measurements of lysosomal pH (to verify the effectiveness of the manipulation) and of cytosolic pH to establish that changes in fura 2 fluorescence are due to changes in $[Ca^{2+}]_c$.

To measure lysosomal pH, incubate cells in culture medium with dextran-conjugates of Texas Red and Oregon Green (pKa 4.7) (0.1 mg/mL of each) for

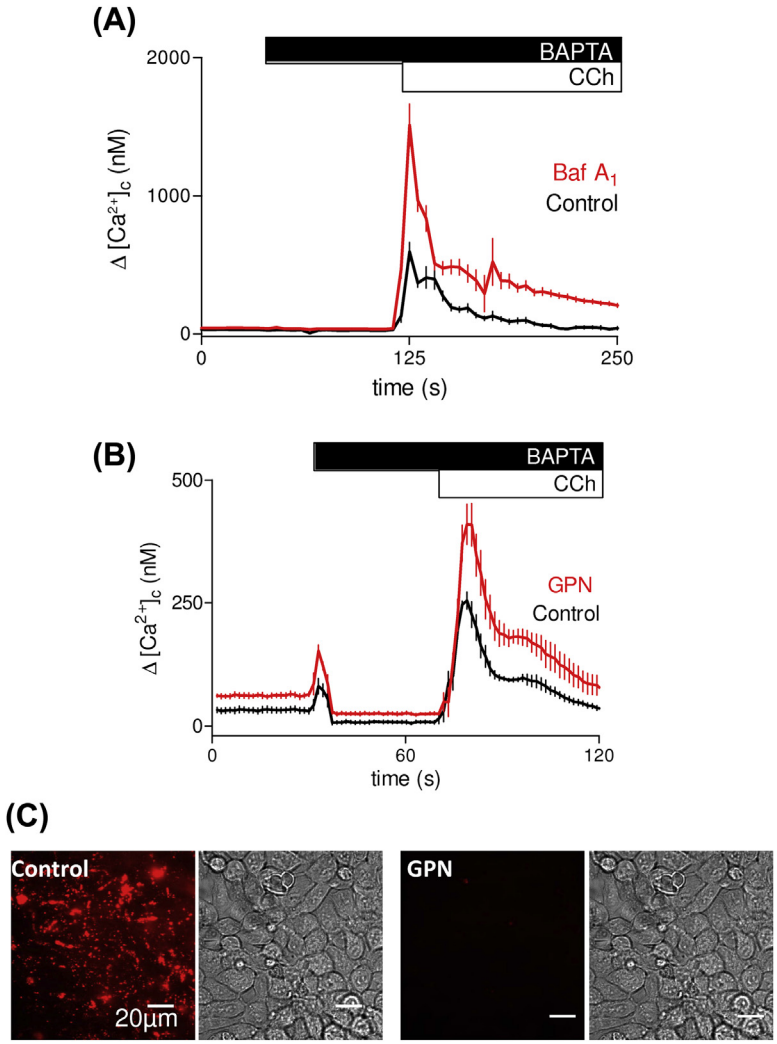

FIGURE 4

Disruption of lysosomes exaggerates the Ca^{2+} signals evoked by carbachol. (A) Fura 2-loaded HEK-293 cells were stimulated with carbachol (CCh, 1 mM) in medium depleted of Ca^{2+} by addition of BAPTA, with or without pre-incubation with bafilomycin A_1 (Baf A_1, 1 μM, 1 h). Results show $[Ca^{2+}]_c$ as means ± SEM from 40 individual cells. (B) Similar analyses of populations of fluo 4-loaded HEK-293 cells with and without treatment with GPN (200 μM, 30 min) and analyzed using a FlexStation III. (C) Effects of the same treatment with GPN on LysoTracker Red staining of HEK-293 cells (left panels) and the corresponding differential interference contrast images (right panels). Panels B and C are reproduced with permission from Lopez Sanjurjo et al. (2013). (See color plate)

12 h at 37 °C, and then for 4 h without the indicators. Wash cells with HBS and record fluorescence (Olympus IX81 microscope with a 40x/1.35 NA objective) using a mercury xenon lamp with alternating filter sets: U-MNIBA (Olympus, excitation 470−495 nm, emission 510−550 nm) and LF561A (Semrock, excitation 550−570 nm, emission 580−630 nm) for Oregon Green and Texas Red, respectively. Capture images at 2-s intervals using an EMCCD camera (Andor iXon 897). To measure cytosolic pH, incubate cells in 96-well plates with SNARF-5F (pKa ~7.2) (Liu, Diwu, & Leung, 2001) (2 μM in DMSO, with Pluronic F127 (0.02%) for 30 min at 20 °C). Illuminate cells (excitation at 561 nm, emission at 580 and 640 nm) using a FlexStation III plate-reader (Section 7), and calibrate emission ratios ($R = F_{580}/F_{640}$) to cytosolic pH (pH_c) from:

$$pH_c = pKa - \log\left[\frac{R - R_b}{R_a - R}\cdot\frac{F_b}{F_a}\right]$$

where Ka is the acid-base dissociation constant for SNARF-5F, and R, R_a and R_b are the emission ratios for the observed measurement and for the fully acidic and fully basic forms of the indicator, respectively. F_a and F_b are the fluorescence intensities (excited at 640 nM) for the fully acidic and basic forms of the indicator. Determine calibration signals by exposing cells for 30 min at the end of the experiment to Ca^{2+}-free cytosol-like medium (CLM) containing nigericin (50 μM), and then replacing it with CLM containing monensin (50 μM) and buffered to different pH values.

7. HIGH-THROUGHPUT ANALYSES OF CYTOSOLIC Ca^{2+} SIGNALS

Single-cell analyses unmask cellular heterogeneity and afford opportunities to examine subcellular Ca^{2+} signals, but they are not easily adapted to quantitative analyses of concentration-effect relationships or high-throughput screening. Rapid measurements of $[Ca^{2+}]_c$ from cells grown in 96-well plates better meet these requirements (Tovey, Sun, & Taylor, 2006). Here we describe the use a FlexStation III 96-well fluorescence plate-reader equipped to allow up to three automated online additions to measure the effects of perturbing lysosomes on the increases in $[Ca^{2+}]_c$ evoked by carbachol in cultured HEK-293 cells. The methods are taken from Lopez Sanjurjo et al. (2013).

7.1 MATERIALS

Most materials are shared with the protocol described in Section 6.

1. Fluo 4-AM (Life Technologies, Paisley, UK)
2. 96-well, black-sided, full-area, assay plates (Greiner, Stonehouse, UK)
3. FlexStation III fluorescence plate-reader (MDS Analytical Devices, Wokingham, UK)

Plate HEK-293 cells (10^5 cells/well) into 96-well plates and use when confluent after ~2 days. Load cells with fluo 4 by incubation with fluo 4-AM (2 μM prepared in anhydrous DMSO, 1 h, 20 °C) in HBS in the dark. Wash cells with HBS, incubate for 1 h to allow de-esterification of the indicator, remove medium and replace with fresh HBS (200 μL). Load the plate into the FlexStation III for experiments. Prepare a sample plate, from which stock solutions (at 2−50x final concentration, depending on protocol; e.g., carbachol, BAPTA, etc.) are withdrawn for automated additions to cells (Tovey et al., 2006). Record fluorescence at 1.4-s intervals (from each column of eight wells before moving to the next column) with excitation at 485 nm and emission at 525 nm. In parallel wells, include additions of Triton X-100 (0.1%, w/v to lyze cells) with $CaCl_2$ (10 mM) or EGTA (10 mM) to provide maximal (F_{max}) and minimal (F_{min}) fluorescence values, respectively. At the end of the experiment, calibrate fluorescence traces to $[Ca^{2+}]_c$ from:

$$\left[Ca^{2+}\right]_c = K_D \frac{F - F_{min}}{F_{max} - F}$$

where F, F_{min}, and F_{max} are the observed, minimal and maximal fluorescence, and K_D is the equilibrium dissociation constant of fluo 4 for Ca^{2+} (345 nM). Data are collected and analyzed using SoftMax Pro and Excel. Figures 4(B) and (C) shows the effects of GPN on both the distribution of LysoTracker Red in HEK-293 cells and the carbachol-evoked increase in $[Ca^{2+}]_c$.

8. TRACKING INTERACTIONS BETWEEN LYSOSOMES AND ER BY FLUORESCENCE MICROSCOPY

Both lysosomes and ER are dynamic organelles (Figure 2(B)), and while electron microscopy provides an informative snapshot of their association in fixed cells (Kilpatrick et al., 2013), it cannot resolve dynamic interactions, and fixation may distort associations. But non-invasive tracking of lysosomes in live cells is challenging: fluorophore bleaching can limit opportunities to capture images for sufficient time and with sufficient temporal resolution; and automated tracking of small dynamic organelles that may leave and re-enter fields of view is demanding. A variety of software, including Volocity (PerkinElmer), MetaMorph (Molecular Devices), ImarisTrack (Bitplane), TrackArt (Matysik & Kraut, 2014) and such ImageJ plugins as Manual Tracking and SpotTracker, allows tracking of mobile fluorophores (Meijering, Dzyubachyk, & Smal, 2012). These programs often rely on user-defined thresholds to guide the software towards analyzing only fluorescent objects of appropriate size, brightness, mobility and lifetime. An obstacle to tracking particles using TIRF microscopy is that particles can move in or out of the illuminated field. However, in our experiments many lysosomes moved relatively slowly along ER tubules and they often remained within the TIRF field. Lysosomes could, therefore, be tracked automatically, using ImarisCell (to identify lysosomes) and ImarisTrack (to track them), over several minutes and their speed (several

μm/min) reliably measured. The methods described, which are adapted from Lopez Sanjurjo (2013), reveal the dynamic relationships between ER and lysosomes (Lopez Sanjurjo et al., 2013) and they allow the movements of individual lysosomes to be quantified (Figure 5).

8.1 MATERIALS

1. Many of the materials required for microscopy are described in Section 6.
2. Imaging dishes, 35-mm diameter with 7-mm No 0 glass insert (MatTek Corporation, Ashland, USA) coated with, poly-L-lysine.
3. Expression plasmids encoding markers for lysosomes (e.g., LAMP1-mCherry or LAMP1-GFP) and ER (e.g., GFP-ER, GFP-IP_3R1, GFP-IP_3R3 or SERCA1-mCherry) are prepared using Maxi DNA purification kits (Qiagen) according to standard methods. The coding sequences of all plasmids must be sequenced.

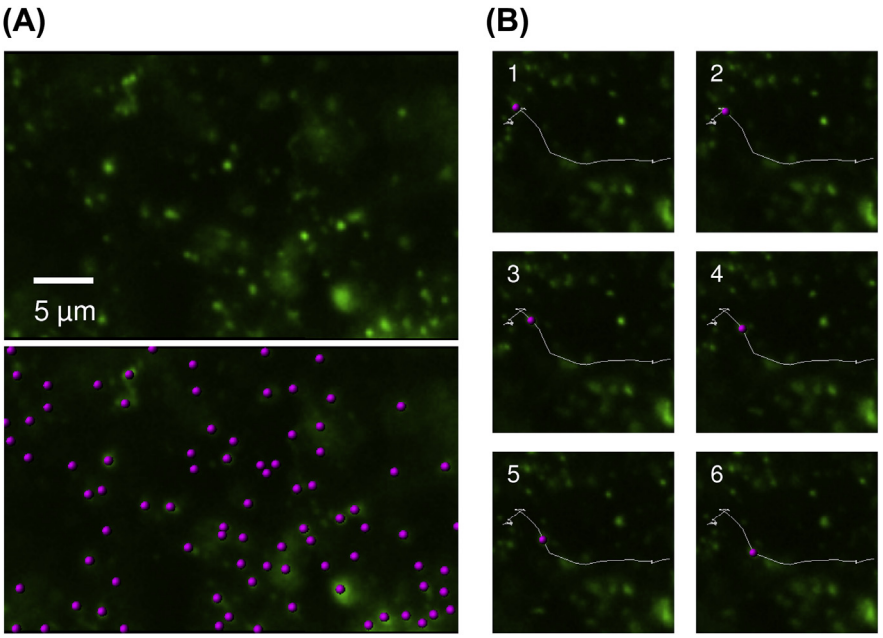

FIGURE 5

Automated identification and tracking of individual lysosomes. (A) Endocytotic loading of COS-7 cells with dextran-conjugated Oregon Green was used to label lysosomes (upper panel). The lysosomes were automatically identified from wide-field images using ImarisCell (violet spheres, lower panel). (B) Tracking of a single lysosome for 3 min (white line). Images (1–6, each separated by 1 s) show the position of the tracked lysosome in six consecutive frames. Scale bar applies to all images. (See color plate)

4. Transit-LT1 transfection reagent (Geneflow). Fibronectin (Millipore). Hank's Balanced Salt Solution (Life Technologies). HBS and Ca^{2+}-free HBS (Section 6)
5. LysoTracker Red DND-99 (Life Technologies)
6. TIRF microscope and tracking analysis software (e.g., Imaris software modules)

Coat glass-bottomed 35-mm culture dishes with human fibronectin (10 μg/mL) or poly-L-lysine (0.01%, w/v) for 1 h. Wash with sterile Hank's Balanced Salt Solution. Seed cells (~2.5 mL/dish) at densities designed to achieve ~50% confluence on the next day. Transiently transfect cells with plasmids 24 h after seeding. For each 35-mm dish, mix DNA (2 μg) with serum-free DMEM/F12 (200 μL). Add Transit-LT1 reagent (5 μL) and mix. Incubate at room temperature for 15−20 min, then add the mixture drop-wise to each dish of cells. Culture cells for 24−48 h before imaging. To load cells with the lysosomal marker LysoTracker Red, incubate cells with LysoTracker Red DND-99 (50 nM) for 1 h at 20 °C, then wash several times with HBS. Use cells immediately.

Prepare cells for imaging by washing dishes with HBS or Ca^{2+}-free HBS. Image cells using a TIRF microscope, such as an Olympus IX81 inverted microscope, with a 60x/1.45 NA or 150x/1.45 NA objective. Illuminate cells with 488-nm (for GFP) or 561-nm (for mCherry and LysoTracker Red) diode lasers (Olympus), using U-MNIBA (Olympus; excitation 470−495 nm, emission 510−550 nm) and LF561A (Semrock; excitation 550−570 nm, emission 580−630 nm) filters, respectively. With the filters used, there should be no significant crosstalk between green and red channels. Lasers should be aligned and focused, before altering their angle of incidence to achieve total internal reflection. Acquire images with an EMCCD camera such as an iXon 897 (Andor Technology), with sufficient speed (>1 Hz) to track lysosomes and ER tubules reliably.

Process images using software such as Cell^R (Olympus) or ImageJ. Correct all images for background fluorescence determined from regions outside cells. Express fluorescence changes from ROI as F/F_0 or $\Delta F/F_0$, where F_0 and F are the average fluorescence at the start of the experiment and at each time point, respectively; $\Delta F = F - F_0$. To track fluorophores use the software described above. We usually use Imaris. Define threshold parameters that isolate fluorescent objects of appropriate size, brightness, mobility and lifetime. For quantitative analyses of the colocalization of two fluorophores, identify background-corrected ROI (~200−400 μm^2) within the peripheral cytoplasm that exclude the nucleus and perinuclear area. Assess the statistical significance of colocalization using the Colocalization Analysis/Colocalization Test plugin (ImageJ) with 100 iterations. Ignore pixels with no fluorescence from either fluorophore (Costes et al., 2004). Quantify colocalization using the same plugin to threshold images and calculate Pearson's correlation coefficient (R_{col}), ignoring pixels with intensities below threshold. $R_{col} = \Sigma(R_i - R_m)(G_i - G_m)/\sqrt{\Sigma(R_i - R_m)^2 \Sigma(G_i - G_m)^2}$, where G_i and R_i are the intensities of individual green and red pixels respectively, and G_m and R_m are the mean intensities of green and red pixels. $R_{col} = 1$ denotes perfect colocalization.

Our tracking experiments demonstrate that many lysosomes associate with ER and move with it (Figure 2(B)) and they demonstrate that it is practicable to

non-invasively track individual lysosomes reliably and with sufficient temporal resolution to provide quantitative analyses of mobility (Figure 5).

CONCLUSIONS

A recurrent theme in Ca^{2+} signaling is the importance of spatially organized Ca^{2+} signals (Berridge, Bootman, & Roderick, 2003). It is becoming increasingly recognized that interactions between intracellular membranes, often facilitated by scaffold proteins or tethers, play important roles in both shaping and decoding these Ca^{2+} signals (Lam & Galione, 2013; Prinz, 2014). Lysosomes are relative latecomers to the community of Ca^{2+} signaling organelles (Morgan et al., 2011), but there is persuasive evidence that they too can both decode and shape cytosolic Ca^{2+} signals. The latter by both sequestering and releasing Ca^{2+} (Brailoiu et al., 2010; Lopez Sanjurjo et al., 2013; Morgan et al., 2013). As for other interactions between Ca^{2+} signaling membranes, the interactions between ER and lysosomes appear to be intimate, and mediated by specific associations between them (Friedman et al., 2013; Kilpatrick et al., 2013). Ca^{2+} release by lysosomes, for example, can selectively trigger Ca^{2+} release, via CICR, from IP_3R and RyR within ER (Brailoiu et al., 2010; Calcraft et al., 2009). Conversely, Ca^{2+} released from the ER is selectively accumulated by lysosomes, while Ca^{2+} entering cells via SOCE is not (Lopez Sanjurjo et al., 2013). Many questions remain unanswered. How do lysosomes accumulate Ca^{2+}? Which lysosomal channels mediate Ca^{2+} release? Do changes in lysosomal pH play important physiological roles in determining lysosomal Ca^{2+} release? How do lysosomes maintain their association with ER for extended periods while each is moving? How are these dynamic interactions regulated? What is the impact of the associations on other aspects of ER and lysosome behaviour? Does defective tethering of ER and lysosomes contribute to lysosomal pathologies?

In this short review, we described methods that allow the contributions of lysosomes to Ca^{2+} signaling to be inferred from measurements of $[Ca^{2+}]_c$ (Sections 6 and 7), but these approaches are indirect. There remains an urgent need to develop Ca^{2+} sensors capable of reliably reporting $[Ca^{2+}]$ within lysosomes. In Section 8, we described how optical microscopy can reveal the dynamics of organelles, including lysosomes. With ever improving optical microscopy (Han et al., 2013) and opportunities to tag endogenous proteins by gene-editing (Kim & Kim, 2014), these methods will provide exciting opportunities to define dynamic relationships between organelles with exquisite spatial and temporal resolution.

ACKNOWLEDGMENTS

Supported by the Biotechnology and Biological Sciences Research Council (L0000075). CWT is a Wellcome Trust Senior Investigator (101844). CIL-S was supported by studentships from Caixa Galicia Foundation and Obra Social La Caixa, Spain.

REFERENCES

Berridge, M. J. (1997). Elementary and global aspects of calcium signalling. *Journal of Physiology, 499*, 291–306.

Berridge, M. J., Bootman, M. D., & Roderick, H. L. (2003). Calcium signalling: dynamics, homeostasis and remodelling. *Nature Reviews: Molecular Cell Biology, 4*, 517–529.

Berridge, M. J., Lipp, P., & Bootman, M. D. (2000). The versatility and universality of calcium signalling. *Nature Reviews: Molecular Cell Biology, 1*, 11–21.

Betzig, E., Patterson, G. H., Sougrat, R., Lindwasser, O. W., Olenych, S., Bonifacino, J. S., et al. (2006). Imaging intracellular fluorescent proteins at nanometer resolution. *Science, 313*, 1642–1645.

Bootman, M. D., Rietdorf, K., Collins, T., Walker, S., & Sanderson, M. (2014). Ca^{2+}-sensitive fluorescent dyes and intracellular Ca^{2+} imaging. In Y. B. Parys, M. D. Bootman, D. I. Yule, & G. Bultynck (Eds.), *Cold Spring Harbor protocols. Calcium techniques a laboratory manual* (pp. 83–99). Cold Spring Harbor Laboratory Press.

Brailoiu, E., Rahman, T., Churamani, D., Prole, D. L., Brailoiu, G. C., Hooper, R., et al. (2010). An NAADP-gated two-pore channel targeted to the plasma membrane uncouples triggering from amplifying Ca^{2+} signals. *Journal of Biological Chemistry, 285*, 38511–38516.

Burgess, G. M., McKinney, J. S., Fabiato, A., Leslie, B. A., & Putney, J. W., Jr. (1983). Calcium pools in saponin-permeabilized guinea pig hepatocytes. *Journal of Biological Chemistry, 258*, 15336–15345.

Calcraft, P. J., Ruas, M., Pan, Z., Cheng, X., Arredouani, A., Hao, X., et al. (2009). NAADP mobilizes calcium from acidic organelles through two-pore channels. *Nature, 459*, 596–600.

Cang, C., Zhou, Y., Navarro, B., Seo, Y. J., Aranda, K., Shi, L., et al. (2013). mTOR regulates lysosomal ATP-sensitive two-pore Na^{+} channels to adapt to metabolic state. *Cell, 152*, 778–790.

Christensen, K. A., Myers, J. T., & Swanson, J. A. (2002). pH-dependent regulation of lysosomal calcium in macrophages. *Journal of Cell Science, 115*, 599–607.

Churchill, G. C., Okada, Y., Thomas, J. M., Genazzani, A. A., Patel, S., & Galione, A. (2002). NAADP mobilizes Ca^{2+} from reserve granules, lysosome-related organelles, in sea urchin eggs. *Cell, 111*, 703–708.

Costes, S. V., Daelemans, D., Cho, E. H., Dobbin, Z., Pavlakis, G., & Lockett, S. (2004). Automatic and quantitative measurement of protein-protein colocalization in live cells. *Biophysical Journal, 86*, 3993–4003.

Demaurex, N., Lew, D. P., & Krause, K.-H. (1992). Cyclopiazonic acid depletes intracellular Ca^{2+} stores and activates an influx pathway for divalent cations in HL-60 cells. *Journal of Biological Chemistry, 267*, 2318–2324.

Dong, X. P., Wang, X., & Xu, H. (2010). TRP channels of intracellular membranes. *Journal of Neurochemistry, 113*, 313–328.

Drose, S., & Altendorf, K. (1997). Bafilomycins and concanamycins as inhibitors of V-ATPases and P-ATPases. *Journal of Experimental Biology, 200*, 1–8.

Exton, J. H. (1980). Mechanisms involved in α-adrenergic phenomena: role of calcium ions in actions of catecholamines in liver and other tissues. *American Journal of Physiology, 238*, E3–E12.

Friedman, J. R., Dibenedetto, J. R., West, M., Rowland, A. A., & Voeltz, G. K. (2013). Endoplasmic reticulum-endosome contact increases as endosomes traffic and mature. *Molecular Biology of the Cell, 24*, 1030–1040.

Gerasimenko, J. V., Tepikin, A. V., Petersen, O. H., & Gerasimenko, O. V. (1998). Calcium uptake via endocytosis with rapid release from acidifying endosomes. *Current Biology, 8*, 1335–1338.

Giepmans, B. N., Adams, S. R., Ellisman, M. H., & Tsien, R. Y. (2006). The fluorescent toolbox for assessing protein location and function. *Science, 312*, 217–224.

Grynkiewicz, G., Poenie, M., & Tsien, R. Y. (1985). A new generation of Ca^{2+} indicators with greatly improved fluorescence properties. *Journal of Biological Chemistry, 260*, 3440–3450.

Han, R., Li, Z., Fan, Y., & Jiang, Y. (2013). Recent advances in super-resolution fluorescence imaging and its applications in biology. *Journal of Genetics and Genomics, 40*, 583–595.

Helle, S. C., Kanfer, G., Kolar, K., Lang, A., Michel, A. H., & Kornmann, B. (2013). Organization and function of membrane contact sites. *Biochimica et Biophysica Acta, 1833*, 2526–2541.

Huang, P., Zou, Y., Zhong, X. Z., Cao, Q., Zhao, K., Zhu, M. X., et al. (2014). P2X4 forms functional ATP-activated cation channels on lysosomal membranes regulated by luminal pH. *Journal of Biological Chemistry, 268*, 17658–17667.

Huynh, C., & Andrews, N. W. (2005). The small chemical vacuolin-1 alters the morphology of lysosomes without inhibiting Ca^{2+}-regulated exocytosis. *EMBO Reports, 6*, 843–847.

Ishida, Y., Nayak, S., Mindell, J. A., & Grabe, M. (2013). A model of lysosomal pH regulation. *Journal of General Physiology, 141*, 705–720.

Jadot, M., Colmant, C., Wattiaux-De Coninck, S., & Wattiaux, R. (1984). Intralysosomal hydrolysis of glycyl-L-phenylalanine 2-naphthylamide. *Biochemical Journal, 219*, 965–970.

Jha, A., Ahuja, M., Patel, S., Brailoiu, E., & Muallem, S. (2014). Convergent regulation of the lysosomal two-pore channel-2 by Mg^{2+}, NAADP, $PI(3,5)P_2$ and multiple protein kinases. *EMBO Journal, 33*, 501–511.

Kilpatrick, B. S., Eden, E. R., Schapira, A. H., Futter, C. E., & Patel, S. (2013). Direct mobilisation of lysosomal Ca^{2+} triggers complex Ca^{2+} signals. *Journal of Cell Science, 126*, 60–66.

Kim, H., & Kim, J. S. (2014). A guide to genome engineering with programmable nucleases. *Nature Reviews: Genetics, 15*, 321–334.

Klemper, M. S. (1985). An adenosine triphosphate-dependent calcium uptake pump in human neutrophil lysosomes. *Journal of Clinical Investigation, 76*, 303–310.

Konieczny, V., Keebler, M. V., & Taylor, C. W. (2012). Spatial organization of intracellular Ca^{2+} signals. *Seminars in Cell & Developmental Biology, 23*, 172–180.

Lakowicz, J. R. (2006). *Principles of fluorescence spectroscopy.* New York: Springer.

Lam, A., & Galione, A. (2013). The endoplasmic reticulum and junctional membrane communication during calcium signaling. *Biochimica et Biophysica Acta, 1833*, 2542–2559.

Lee, H. C. (2005). Nicotinic acid adenine dinucleotide phosphate (NAADP)-mediated calcium signaling. *Journal of Biological Chemistry, 280*, 33693–33696.

Lemons, R. M., & Thoene, J. G. (1991). Mediated calcium transport by isolated human fibroblast lysosomes. *Journal of Biological Chemistry, 266*, 14378–14382.

Lewis, R. S. (2012). Store-operated calcium channels: new perspectives on mechanism and function. *Cold Spring Harbor Perspectives in Biology, 3*, a003970.

Li, W., Schultz, C., Llopis, J., & Tsien, R. Y. (1997). Membrane-permeant esters of inositol polyphosphates, chemical syntheses and biological applications. *Tetrahedron, 53*, 12017–12040.

Liu, J., Diwu, Z., & Leung, W. Y. (2001). Synthesis and photophysical properties of new fluorinated benzo[c]xanthene dyes as intracellular pH indicators. *Bioorganic and Medicinal Chemistry Letters, 11*, 2903–2905.

Lloyd-Evans, E., Morgan, A. J., He, X., Smith, D. A., Elliot-Smith, E., Sillence, D. J., et al. (2008). Niemann-Pick disease type C1 is a sphingosine storage disease that causes deregulation of lysosomal calcium. *Nature Medicine, 14*, 1247–1255.

Lopez Sanjurjo C.I. (2013). *Lysosomes shape cytosolic Ca^{2+} signals by selectively sequestering Ca^{2+} released from the endoplasmic reticulum* (Ph.D. thesis). University of Cambridge.

Lopez Sanjurjo, C. I., Tovey, S. C., Prole, D. L., & Taylor, C. W. (2013). Lysosomes shape Ins(1,4,5)P_3-evoked Ca^{2+} signals by selectively sequestering Ca^{2+} released from the endoplasmic reticulum. *Journal of Cell Science, 126*, 289–300.

Lytton, J., Westlin, M., Burk, S. E., Shull, G. E., & MacLennan, D. H. (1992). Functional comparisons between isoforms of the sarcoplasmic or endoplasmic reticulum family of calcium pumps. *Journal of Biological Chemistry, 267*, 14483–14489.

Mackrill, J. J. (2010). Ryanodine receptor calcium channels and their partners as drug targets. *Biochemical Pharmacology, 79*, 1535–1543.

Marchant, J., Callamaras, N., & Parker, I. (1999). Initiation of IP_3-mediated Ca^{2+} waves in *Xenopus* oocytes. *EMBO Journal, 18*, 5285–5299.

Marshansky, V., & Futai, M. (2008). The V-type H^+-ATPase in vesicular trafficking: targeting, regulation and function. *Current Opinion in Cell Biology, 20*, 415–426.

Martin-Fernandez, M. L., Tynan, C. J., & Webb, S. E. (2013). A 'pocket guide' to total internal reflection fluorescence. *Journal of Microscopy, 252*, 16–22.

Matysik, A., & Kraut, R. S. (2014). TrackArt: the user friendly interface for single molecule tracking data analysis and simulation applied to complex diffusion in mica supported lipid bilayers. *BMC Research Notes, 7*, 274.

Meijering, E., Dzyubachyk, O., & Smal, I. (2012). Methods for cell and particle tracking. *Methods in Enzymology, 504*, 183–200.

Michelangeli, F., & East, J. M. (2011). A diversity of SERCA Ca^{2+} pump inhibitors. *Biochemical Society Transactions, 39*, 789–797.

Morgan, A. J., Davis, L. C., Wagner, S. K., Lewis, A. M., Parrington, J., Churchill, G. C., et al. (2013). Bidirectional Ca^{2+} signaling occurs between the endoplasmic reticulum and acidic organelles. *Journal of Cell Biology, 18*, 789–805.

Morgan, A. J., & Galione, A. (2007). NAADP induces pH changes in the lumen of acidic Ca^{2+} stores. *Biochemical Journal, 402*, 301–310.

Morgan, A. J., Platt, F. M., Lloyd-Evans, E., & Galione, A. (2011). Molecular mechanisms of endolysosomal Ca^{2+} signalling in health and disease. *Biochemical Journal, 439*, 349–374.

Nagai, T., Yamada, S., Tominaga, T., Ichikawa, M., & Miyawaki, A. (2004). Expanded dynamic range of fluorescent indicators for Ca^{2+} by circularly permuted yellow fluorescent proteins. *Proceedings of the National Academy of Sciences USA, 101*, 10554–10559.

Patel, S., & Docampo, R. (2010). Acidic calcium stores open for business: expanding the potential for intracellular Ca^{2+} signaling. *Trends in Cell Biology, 20*, 277–286.

Patel, S., Ramakrishnan, L., Rahman, T., Hamdoun, A., Marchant, J. S., Taylor, C. W., et al. (2011). The endo-lysosomal system as an NAADP-sensitive acidic Ca^{2+} store: role for the two-pore channels. *Cell Calcium, 50*, 157–167.

Pierzynska-Mach, A., Janowski, P. A., & Dobrucki, J. W. (2014). Evaluation of acridine orange, LysoTracker Red, and quinacrine as fluorescent probes for long-term tracking of acidic vesicles. *Cytometry A, 85*, 729–737.

Pitt, S. J., Lam, A. K., Rietdorf, K., Galione, A., & Sitsapesan, R. (2014). Reconstituted human TPC1 is a proton-permeable ion channel and is activated by NAADP or Ca^{2+}. *Science Signaling, 7*, ra46.

Prinz, W. A. (2014). Bridging the gap: membrane contact sites in signaling, metabolism, and organelle dynamics. *Journal of Cell Biology, 205*, 759–769.

Putney, J. W., Jr. (1997). *Capacitative calcium entry.* Austin, Texas, USA: R.G.Landes Company.

Ringer, S. (1883). A further contribution regarding the influence of the different constituents of the blood on the contraction of the heart. *Journal of Physiology, 4*, 29–42.

Rizzuto, R., Brini, M., Murgia, M., & Pozzan, T. (1993). Microdomains with high Ca^{2+} close to IP_3-sensitive channels that are sensed by neighbouring mitochondria. *Science, 262*, 744–747.

Rizzuto, R., De Stefani, D., Raffaello, A., & Mammucari, C. (2012). Mitochondria as sensors and regulators of calcium signalling. *Nature Reviews: Molecular Cell Biology, 13*, 566–578.

Sagara, Y., & Inesi, G. (1991). Inhibition of the sarcoplasmic reticulum Ca^{2+} transport ATPase by thapsigargin at subnanomolar concentrations. *Journal of Biological Chemistry, 266*, 13503–13506.

Saleem, H., Tovey, S. C., Molinski, T. F., & Taylor, C. W. (2014). Interactions of antagonists with subtypes of inositol 1,4,5-trisphosphate (IP_3) receptor. *British Journal of Pharmacology, 171*, 3298–3312.

Seo, M.-D., Velamakanni, S., Ishiyama, N., Stathopulos, P. B., Rossi, A. M., Khan, S. A., et al. (2012). Structural and functional conservation of key domains in $InsP_3$ and ryanodine receptors. *Nature, 483*, 108–112.

Shim, S. H., Xia, C., Zhong, G., Babcock, H. P., Vaughan, J. C., Huang, B., et al. (2012). Super-resolution fluorescence imaging of organelles in live cells with photoswitchable membrane probes. *Proceedings of the Academy of Natural Sciences of the United States of America, 109*, 13978–13983.

Shuai, J., & Parker, I. (2005). Optical single-channel recording by imaging Ca^{2+} flux through individual ion channels: theoretical considerations and limits to resolution. *Cell Calcium, 37*, 283–299.

Smith, I. F., & Parker, I. (2009). Imaging the quantal substructure of single IP_3R channel activity during Ca^{2+} puffs in intact mammalian cells. *Proceedings of the National Academy of Sciences of the United States of America, 106*, 6404–6409.

Streb, H., Irvine, R. F., Berridge, M. J., & Schulz, I. (1983). Release of Ca^{2+} from a nonmitochondrial intracellular store in pancreatic acinar cells by inositol-1,4,5-trisphosphate. *Nature, 306*, 67–69.

Suzuki, J., Kanemaru, K., Ishii, K., Ohkura, M., Okubo, Y., & Iino, M. (2014). Imaging intraorganellar Ca^{2+} at subcellular resolution using CEPIA. *Nature Communications, 5*, 4153.

Tang, S., Wong, H. C., Wang, Z. M., Huang, Y., Zou, J., Zhuo, Y., et al. (2011). Design and application of a class of sensors to monitor Ca^{2+} dynamics in high Ca^{2+} concentration cellular compartments. *Proceedings of the National Academy of Sciences of the United States of America, 108*, 16265–16270.

Taylor, C. W., & Dale, P. (2012). Intracellular Ca^{2+} channels – a growing community. *Molecular and Cellular Endocrinology, 353*, 21–28.

Tovey, S. C., Dedos, S. G., Taylor, E. J. A., Church, J. E., & Taylor, C. W. (2008). Selective coupling of type 6 adenylyl cyclase with type 2 IP_3 receptors mediates a direct sensitization of IP_3 receptors by cAMP. *Journal of Cell Biology, 183*, 297–311.

Tovey, S. C., Goraya, T. A., & Taylor, C. W. (2003). Parathyroid hormone increases the sensitivity of inositol trisphosphate receptors by a mechanism that is independent of cyclic AMP. *British Journal of Pharmacology, 138*, 81–90.

Tovey, S. C., Sun, Y., & Taylor, C. W. (2006). Rapid functional assays of intracellular Ca^{2+} channels. *Nature Protocols, 1*, 259–263.

Vais, H., Foskett, J. K., & Mak, D. O. (2010). Unitary Ca^{2+} current through recombinant type 3 $InsP_3$ receptor channels under physiological ionic conditions. *Journal of General Physiology, 136*, 687–700.

Van der Kant, R., & Neefjes, J. (2014). Small regulators, major consequences – Ca^{2+} and cholesterol at the endosome-ER interface. *Journal of Cell Science, 127*, 929–938.

Wang, X., Zhang, X., Dong, X. P., Samie, M., Li, X., Cheng, X., et al. (2012). TPC proteins are phosphoinositide-activated sodium-selective ion channels in endosomes and lysosomes. *Cell, 151*, 372–383.

Wozniak, M. J., Bola, B., Brownhill, K., Yang, Y. C., Levakova, V., & Allan, V. J. (2009). Role of kinesin-1 and cytoplasmic dynein in endoplasmic reticulum movement in VERO cells. *Journal of Cell Science, 122*, 1979–1989.

Yoshimori, T., Yamamoto, A., Moriyama, Y., Futai, M., & Tashiro, Y. (1991). Bafilomycin A_1, a specific inhibitor of vacuolar-type H^+-ATPase, inhibits acidification and protein degradation in lysosomes of cultured cells. *Journal of Biological Chemistry, 266*, 17707–17712.

Zhang, J., Campbell, R. E., Ting, A. Y., & Tsien, R. Y. (2002). Creating new fluorescent probes for cell biology. *Nature Reviews: Molecular Cell Biology, 3*, 906–918.